ON-LINE VISUAL INSPECTION OF CONTINUOUS CAST METALLIC STRIP SURFACE

Carlos Fernández[*], Carlos Platero[*], Patrick Alvarez[†], Pascual Campoy[*], Rafael Aracil[*]

Abstract

A visual inspection system architecture for detecting and analyzing surface defects in continuous cast metallic strip is described. Real-time performance requirements has forced up the development of a high-parallel architecture for high-speed image processing. Matricial cameras are used for image acquisition instead of linear ones because of the surface appearance. Inspection is achieved with 1mm^2 resolution. Similarity-based algorithms as well as texture algorithms have been developed and hardware-implemented for defect detection in a high-textured surface where, for the most of defects, segmentation can not be achieved by only means of threshold techniques. The system has been applied to continuous cast aluminum inspection, where up to fifteen different kinds of defects must be detected and classified.

1 Introduction

Surface inspection is usually a bottle-neck in many production processes[1]. There is a great number of manufacturing processes where inspection for surface finishing or surface defects is attempted: steel strip, hot steel slabs, plastic plates, painted surfaces, wooden surfaces, profiles,...[2]. The most difficult task of inspection is that of inspecting for visual appearance[1]. The visual inspection in most manufacturing processes depends mainly on human inspectors. The human visual system is adapted to perform in a world of variety and change; the visual inspection process, on the other hand, requires observing the same type of image repeatedly to detect anomalies. The accuracy of human visual inspection declines with dull, endlessly routine jobs. Slow, expensive, erratic inspection is the result. Automated visual inspection is obviously the alternative to the human inspector.

(*) Dept. of Systems and Electronics (DISAM). Polytechnical Univ. of Madrid, Spain.
Tel: +34-1-336 30 61 Fax: +34-1-564-29-61 E-mail: cfernandez@disam.upm.es

(†) ICPI, Catholic Univ. of Lyon, France, presently at DISAM.

The inspection of smooth surfaces is a quite easy task[3], since it can be done by selecting an adequate global threshold level. For rough surfaces more sophisticated algorithms are needed. These algorithms should include segmentation techniques based on similarity operators like neighborhood average, or texture techniques that consider not only deviation in gray level from a pattern but also changes in the spatial distribution of pixel intensities. Cast metal surfaces appear as textured surfaces, have a high reflection coefficient[4] and move fast under the inspection devices, which make difficult to achieve visual inspection with image processing equipment.

2 Specifications for the Visual Inspection Task

Specifications for the vision system related to resolution, processing time and operating mode are determined by the minimum size of defects, production rate and frequency of defects, which are respectively:

*Minimum size of defects: 1 mm^2. This forces up a minimum resolution of 2 pixels/mm[5].

*Production specifications: Two-sides inspection for a 1680 mm wide aluminum strip at 2 m/s speed.

*Defects can appear at any time; they can be as small as 1 mm^2 or they can have thousands of square millimeters extensions and appear only in a very small portion of the strip or they can appear along large portions of the strip during a lot of minutes. The detection of defect, as well as its measurement for after classification must be done on-line; i.e., no images containing defects can be stored for off-line processing.

Specifications also include the necessity of modularity of the developed system, that is, it should permit to use the number of cameras required by the application -depending on the resolution necessities and on the geometry of the surface to inspect- as well as it should permit parallelism for higher performance, if needed.

3 Visual Inspection System

An artificial vision system specially developed for surface inspection of flat continuous products has been developed; it includes: Lighting system; Image acquisition devices; Defect detection module; Surface finishing measurement module and Feature extraction module.

3.1 Lighting System

Defects over metallic surfaces are characterized by alterations in the surface micro-structure. At the boundary between air and metal light scatters; light streaking the boundary is either transmitted or reflected; if the boundary is very smooth the light is scattered very little; if it is rough light is scattered in all directions[4] Since defect appearing in metallic surfaces involve material alterations, seeking for the specular component of the reflected light would result in a defect detection when the

amount of scattered light vary due to surface alterations.
A light simulator has been developed to obtain the optimum configuration for the lighting system geometry. Instead of physical optics models from Beckman-Spizzichino[7] -that show not very suitable when the wavelength of incident light is not depreciable in front of the dimensions of surface imperfections- geometrical optics models from Torrance-Sparrow [8] [9] are used.
Specular reflection from rough surfaces should be modeled by means of reflectance models, i. e., using geometrical optics, which use the short wavelength of light to simplify the analysis of the reflection problem. Rough surfaces -cast metallic surfaces belong to this group- scatters light in many directions, more in casting direction than in others. To mathematically modelate this kind of surface - surface with random irregularities- the surface has been described by a statistical distribution of its height to respect a mean level, h, which has been considered zero.
With this model, three kinds of reflection components: diffuse reflection halo, specular reflection halo and specular spike can be observed. Diffuse reflection halo does not significantly change as defects appear on the surface but specular reflection halo and specular spike do; so, seeking for these two reflection components result in an optimum defect enhancing.
Simulator has been programmed using Microsoft C Compiler and the geometry for the lighting system is obtained from it.

3.2 Image Acquisition

Although linear CCD cameras are usually employed when high-speed surface inspection is attempted, matrix CCD cameras has been adopted as more suitable for this application for two main reasons: strip speed up to 2 m/sec. which permits to use acquisition times up to 10 msec. and the necessity of neighborhood processing, since cast metals appear as a high-textured surface which do not permits threshold processing -the most advantage of linear cameras-. Medium resolution -752 by 528 pixels- CCD cameras has been adopted; each camera covers about 370 mm width by 260 mm in the casting direction.

3.3 Defect Detection Module

Each incoming image is locally analyzed in order to detect two kinds of abnormal situations:
*High spatial frequency spots detection (small clear or dark spots).
*Low spatial frequency defect detection (areas with a different spatial distribution of gray levels).
Local analysis is necessary since aluminum surface shows high roughness; clear spots appear mixed with dark ones; several defects do not produce significant variation in absolute gray level values but they produce alterations in the spatial distribution of clear and dark pixels. Although some simple algorithms were firstly developed, their performance was improved by the one exposed in following.

3.3.1 Light pattern and local average

A more sophisticated algorithm has been developed which considers non-uniform light distribution -

intensity distribution- over the aluminum strip. This algorithm permits to process raw incoming images without gray-level correction. Since algorithm performance depends on its real-time execution the least operations have been programmed; these include:

*Neighborhood averaging with NxM kernel; several kernels have been tested; depending on surface roughness -which depends on the aluminum alloy used- 3x3 to 9x12 kernels have shown suitable. The central element of the kernel has been more weighted than others to permit high spatial frequency defect detection as well as low spatial frequency defect detection.

*Local comparison of averaged image with light pattern (local_average_gray_level +/- 3σ). This permits independent segmentation of "clear" and "dark" defects in incoming images.

*Morphological operations are then executed for noise reduction; these consist on north-south and west-east connectivity.

This result in a defect detection where segmented defects appear as separated two-class objects, clear or dark. Noise avoidance permits to segment only those objects clearly belonging to defective zones of the aluminum strip which results in low number of objects for each of the defects seen by the cameras, with the correspondent time saving when analyzing them.

A pattern image from the light level over the aluminum strip is continuously actualized after each image processing cycle; this technique avoids problems derived from lamps ageing, dust, variation in the camera optics or variation in the environment light level.

In illustration 1 a real defect detection is shown. On the left, the image from the aluminum strip is shown; the defect corresponds to an opaque band sample. In the center, the segmented defect appears and on the right, objects that compose the defect are shown. Objects appear enclosed in rectangles that consider extreme points position. Although not seen, objects appear labelled from 1 to 255.

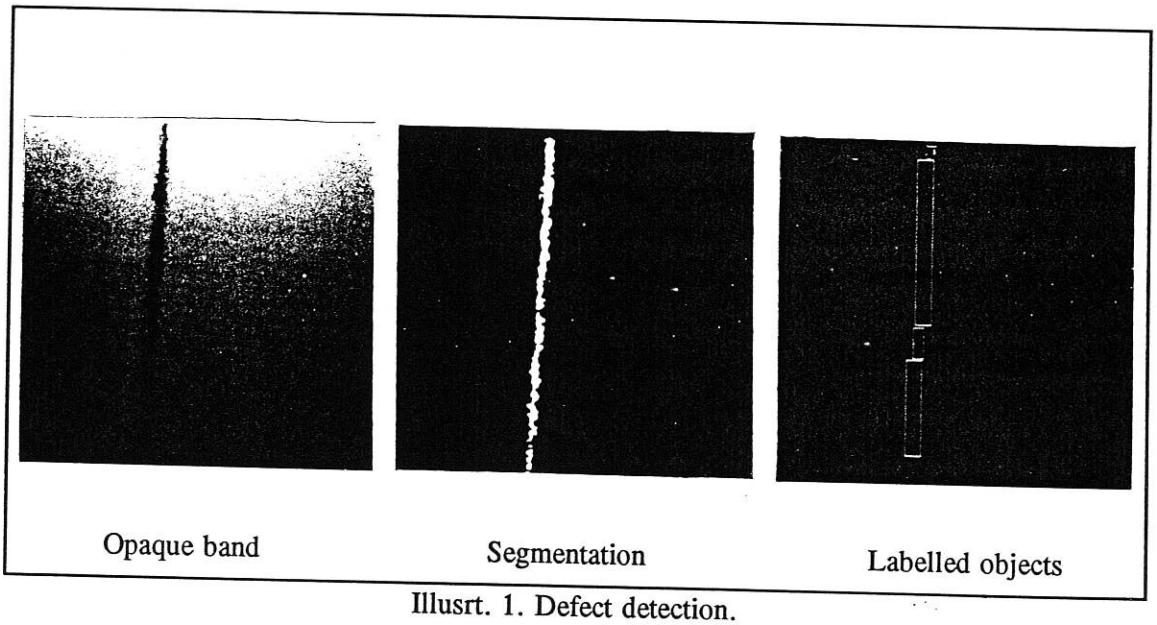

Illusrt. 1. Defect detection.

3.4 Surface finishing measurement

Due to process reasons, like aluminum alloy used or casting rolls wearing, roughness in aluminum surface can vary from 65 microinchs when rolling cylinders are new to 100 microinchs when rolling cylinders need to be substituted. When roughness reaches 75 microinchs the system must notice that. This roughness increase often happens along time as the rolling cylinders wear; nevertheless alterations in surface finishing may appear at any time during the casting process.

Developed algorithms for surface finishing determination are base on texture analysis[10]. Although roughness is not essentially a visual characteristic[11] but a tactile one, human inspectors notice a more rougher surface because the tonal primitives that form it present a higher difference among maximum and minimum values than a less rougher one.

Some gray level difference (GLD)[12] algorithms have been developed and they are actually performing well under normal resolution images, that is, no zoomed images are needed.

Given an incoming image $\mathbf{I=g(x,y)}$ and a displacement vector $\mathbf{d=(N,M)}$ a new image is obtained $\mathbf{gd(x,y)= g(x,y)-g(x+N,y+M)}$.

Two measures are made then over the resulting image: roughness and contrast; the addition of both measures results in a only measure indicating the aluminum surface finishing.

All this processing is made on-line with every incoming image which permits to detect any alteration that may occur. In the normal situation of rolling cylinders wearing, the system warnings when the maximum roughness is reached.

3.5 Feature extraction

Feature extraction, since it concerns objects, requires image labelling. Among used labelling methods, "a simple and effective method of labelling of binary images is by examining the connectivity of pixels with their neighbors and labelling the connected sets"[3].

The "segment labelling" method developed is based on the same principle that the "pixel labelling"[3] one, but it necessitates less access to the features table.

A segment is considered as a set of same-class, same-row and connected pixels, which right and left neighbors are background pixel, other-class pixel or image border.

Scanning the three-level image -dark objects, clear objects and background- left to right and top to bottom, the different segments are detected and each segment is labelled by examining its top neighbors:

* if all the top neighbors are background or other-class pixels, then a new object is created. Its features are the segment ones.
* else, the segment is assigned to the object corresponding to the smallest same-class label met. The other same-class objects met are linked to it. Once the segment is labelled, the corresponding object features are up-dated, depending on the segment ones.

By scanning only top neighbors, "4-connectivity"[13] is considered.

Computing gravity-centers coordinates requires a second local pass over labelled objects. It's based

on vertical and horizontal profiles property as shown in equation 1.
Figure 1 shows labelling algorithm. In figure 2 feature table updating is shown.(Times for 128x128 image. Results correspond to defect shown in illustration 2).

```
Procedure PROCESS_IMAGE :
{ Initialise Label[Light] and Label[Dark]
  LABEL_IMAGE
  COMPUTE_GRAVITY-CENTERS
  UP-DATE_TABLES
}

Procedure LABEL_IMAGE :
{ FOR k=1 TO NR DO
   FOR EACH S_i,j,k DO
   { T=Label[t]
     IF (k!=1), FOR x=i TO j DO
      IF ((L[x,k-1]!=0)
      AND (L[x,k-1]!=T)
      AND (L[x,k-1] same class than T))
      { m=MAX(L[x,k-1],T)
        n=MIN(L[x,k-1],T),
        Link[m]=n
        T=n
      }
     IF (T==Label[t])
     THEN
      CREATE_NEW_OBJECT
     ELSE
      UP-DATE_OBJECT
     FOR x=i TO j DO
      L[x,k]=T
   }
}

Procedure CREATE_NEW_OBJECT :
{ Link[T]=T
  Area[T]=(j-i+1)
  x_min[T]=i
  x_max[T]=j
  y_min[T]=k
  y_max[T]=k
  Increment Label[t]
}

Procedure UP-DATE_OBJECT :
{ Area[T]=Area[T]+(j-i+1)
  x_min[T]=MIN(x_min[T],i)
  x_max[T]=MAX(x_max[T],j)
  y_max[T]=k
}

Procedure COMPUTE_GRAVITY-CENTERS :
{ FOR EACH OBJECT n DO
   { hist=0, x=x_min
     REPEAT
      { FOR y=y_min TO y_max DO
        IF L[x,y]=n THEN hist++
        x++
      }
     WHILE (hist<Area[n]/2)
     x_G[n]=x-1
     <<< idem for y_G >>>
   }
}

Procedure UP-DATE_TABLE :
FOR EACH OBJECT n, FROM THE LAST TO THE FIRST, DO
{ l=Link[n]
  IF (l!=n)
  THEN
   { x_G[l]=(Area[l]*x_G[l]+Area[n]*x_G[n])/(Area[l]+Area[n])
     y_G[l]=(Area[l]*y_G[l]+Area[n]*y_G[n])/(Area[l]+Area[n])
     Area[l]=Area[l]+Area[n]
     x_min[l]=MIN(x_min[l],x_min[n])
     x_max[l]=MAX(x_max[l],x_max[n])
   }

L(x,y) : labelled image.
S_i,j,k : segment of class t, in row k, from column i to column j.
NR : number of rows.
```

Fig. 1. Labelling algorithm.

$$\int_{x_{min}}^{x_G} P_x(x)dx = \int_{y_{min}}^{y_G} P_y(y)dy = \frac{Area}{2}$$

$P_x(x)$: *horizontal profile function*
$P_y(y)$: *vertical profile function*

Eq. 1. Gravity center calculation.

```
OBJECT n°1 :
  Area = 491
  Enclosing Rectangle = [(55;1),(73;47)]
  North exit points = [(61;1),(71;1)]
  South exit points = NONE
  East exit points = NONE
  West exit points = NONE
  Gravity Center = (65;22)
NOT LINKED

OBJECT n°2 :
  Area = 2765
  Enclosing Rectangle = [(28;53),(96;126)]
  North exit points = NONE
  South exit points = [(28;126),(0;126)]
  East exit points = NONE
  West exit points = NONE
  Gravity Center = (66;105)
NOT LINKED

OBJECT n°3 :
  Area = 271
  Enclosing Rectangle = [(64;56),(90;75)]
  North exit points = NONE
  South exit points = NONE
  East exit points = NONE
  West exit points = NONE
  Gravity Center = (78;71)
LINKED TO OBJECT N°2

OBJECT n°4 :
  Area = 25
  Enclosing Rectangle = [(85;60),(89;68)]
  North exit points = NONE
  South exit points = NONE
  East exit points = NONE
  West exit points = NONE
  Gravity Center = (89;66)
LINKED TO OBJECT N°3

OBJECT n°5 :
  Area = 155
  Enclosing Rectangle = [(34;77),(56;94)]
  North exit points = NONE
  South exit points = NONE
  East exit points = NONE
  West exit points = NONE
  Gravity Center = (42;90)
LINKED TO OBJECT N°2

Processing time : 25.05 ms
```

Features before up-dating

```
OBJECT n°1 :
  Area = 491
  Enclosing Rectangle = [(55;1),(73;47)]
  North exit points = [(61;1),(71;1)]
  South exit points = NONE
  East exit points = NONE
  West exit points = NONE
  Gravity Center = (65;22)

OBJECT n°2 :
  Area = 3216
  Enclosing Rectangle = [(28;53),(96;126)]
  North exit points = NONE
  South exit points = [(28;126),(0;126)]
  East exit points = NONE
  West exit points = NONE
  Gravity Center = (66;101)

OBJECT n°3 : (IGNORE IT NOW !)
  Area = 296
  Enclosing Rectangle = [(64;56),(90;75)]
  North exit points = NONE
  South exit points = NONE
  East exit points = NONE
  West exit points = NONE
  Gravity Center = (79;71)

OBJECT n°4 : (IGNORE IT NOW !)
  Area = 25
  Enclosing Rectangle = [(85;60),(89;68)]
  North exit points = NONE
  South exit points = NONE
  East exit points = NONE
  West exit points = NONE
  Gravity Center = (89;66)

OBJECT n°5 : (IGNORE IT NOW!)
  Area = 155
  Enclosing Rectangle = [(34;77),(56;94)]
  North exit points = NONE
  South exit points = NONE
  East exit points = NONE
  West exit points = NONE
  Gravity Center = (42;90)

Total processing time : 25,06 ms
```

Features after up-dating

Fig. 2. Feature table updating.

Illustration 2 shows labelling result. On the left, a defect as seen by cameras; on the right, labelled defect.

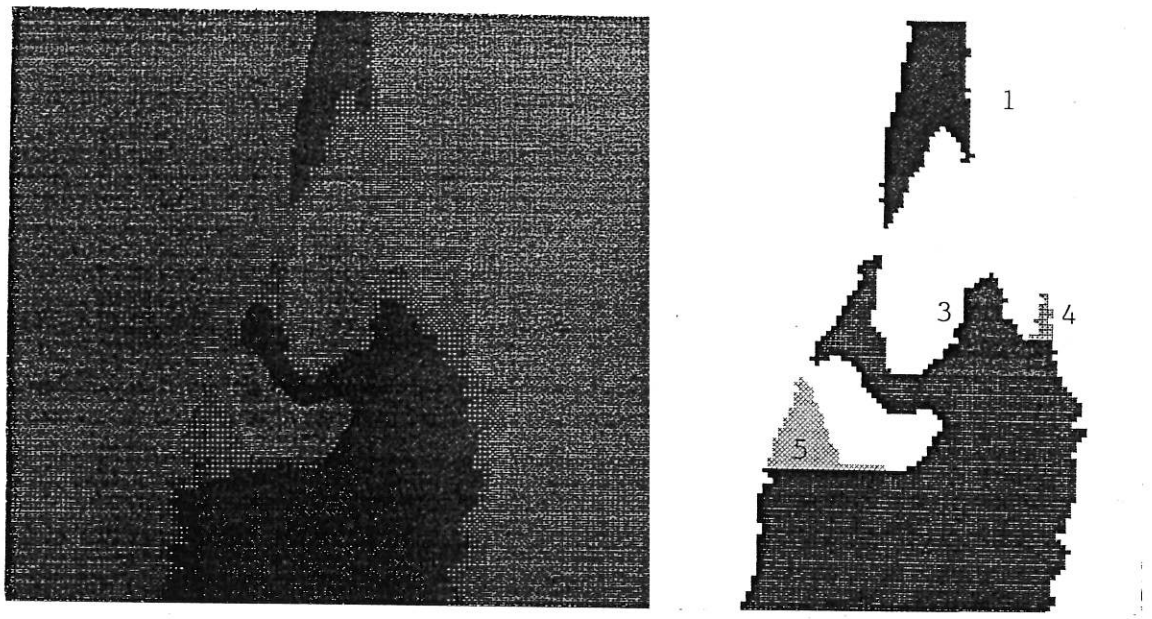

Illustr. 2. Labelling sample.

4 Defect Classification

Every defect is composed by a set of different segmented objects. Once the vision system extracts those features corresponding to all objects from a defective zone of the aluminum strip -low level data-, these features are sent to the Data Base. Afterwards the Expert System will classify them into categories corresponding to different types of defects.

Classification is based upon two data sets: in one hand information about defect visual appearance -as seen by cameras once they have been enhanced- and in the other hand low level data from feature extraction.

Figure 3 shows visual appearance of defects. From this information a general searching tree is proposed, as shown in figure 4.

Structural approach is applied, since heuristic knowledge about defects is available[14]. In this approach searching trees are the basis for classification, since it represents the basic pattern for grammars associated to each defect type. Two separate classification approaches have been carried out: rule-based methods and theoretical decision methods.

First approach is based upon syntactic methods[15]. Its basic principles consist of basic structural patterns definition jointly with determination of rules that govern their interconnection.

Under this approach a medium level qualitative information is derived from low level data -extracted features from objects- which should constitute primitives or terminal elements of the grammar associated to each defect type. The set of rules that applies over this grammar should permit to know if resultant sentence belongs to some defect type, when applied over terminal elements.

PIPES
Appearance: Brilliant longitudinal lines (0.5 mm thick)

ABNORMAL CRYSTALLIZATION
Appearance: Longitudinal opaque bands

SURFACE ROUGHNESS
Appearance: Brilliant spots spread over the surface

LACKS
Appearance: Small-> Brilliant slim objects
Large -> Clear speckles

HOT LINES
Appearance: Longitudinal opaque bands

STICKING
Appearance: Clear speckles due to surface alteration
Dark speckles due to strip distortion

SURFACE INCLUSIONS
Appearance: Dark spots (0.5 - 3 mm diameter)

LEVEL LINES
Appearance: Traversal faint lines

Fig. 3. Visual appearance of main defects.

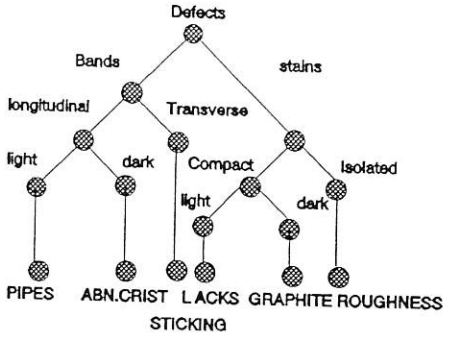

Fig. 4. Searching tree.

Second approach, theoretical decision, considers every defect as formed by a set of objects, being each object represented by a vector: $X_i = object_i = (x_1, x_2, \ldots, x_n)^T$, where x_i represents the numerical value of one of the following features:

- Area.
- Gravity center coordinates.
- Gray level.
- Enclosing rectangle coordinates.
- Connections.

the classification task would consist of obtaining the discriminant functions $d_1(X)$, $d_2(X)$, ...,$d_m(X)$ in a way that an object X^* belongs to class W_i if $d_i(X^*) > d_j(X^*)$; $j = 1, 2, \ldots, m$; $j != i$.
The obtention of this discriminat functions has been entrusted to a Neural Network. Supervised learning algorithms has been tried with good performance -up to 95% recognition rate- with known defects; at this point unsupervised training algorithms are being attempted which should permit to notice the appearance of new defect types as they overcome along the production process; on-line training is the goal of this stage.

4.1. Rule-based approach

A set of G_i grammars is generated in a way that it is possible to stablish relation between sentences

-terminal elements chains- with defect types, w_i. A free context grammar[16][17] has been used $G_i=(V_{N,i}, V_{T,i}, S_i, F_i)$ $0<i<7$ where:

- $V_{N,i}$: Finite set of non terminal elements for grammar i.
- $V_{T,i}$: Finite set of terminal elements for grammar i.
- S_i: Initial starting symbol belonging to $V_{N,i}$.
- F_i: Finite set of production rules for grammar i.

As resulting from defect segmentation algorithm, defects appear fragmented into multiple objects; the first problem to solve is to associate these objects into coherent terminal elements. This is obtaining by object ordering by their area; every object is then classified by means of its shape -points, speckles, longitudinal bands and traversal bands-. next, associations between terminal elements and objects are stablished starting from those more significant objects -the so called seeds-. Finally, terminal elements so obtained are labelled with medium level characteristics[18]:

- Dark Traversal Bands (DTB).
- Clear Traversal Bands (CTB).
- Dark Longitudinal Bands (DLB).
- Clear Longitudinal Bands (CLB).
- Dark Speckles (DS).
- Clear Speckles (CS).
- Isolated Dark Points (IDP).
- Isolated Clear Points (ICP).

For each defect type a data tree is obtained where each node represents terminal elements and low level data concerning each of the areas that compose the whole defect. Rules from every grammar are applied over this tree to determine which defect type does it belong to.

5 Prototype and Results

Visual inspection algorithms have been developed using a commercial image processing board from MATROX (IMAGE-1280 Board with real-time capabilities -up to 1000 MIPS on pipelined processing-).

For prototype implementation a Digital Signal Processor from ANALOG DEVICES (ADSP-21020) has been used by its significant lower cost. Since its lower performance parallel processing is achieve by means of attaching two cameras to each processing board. Five boards are attached together by means of a RS-422 link which connects the whole set to a host computer entrusted of data collection -features extracted from every detected defect- in order to classify them and to afterwards take control actions over the casting process. Figure 5 shows a typical message from image processor boards. The whole process -image acquisition, defect detection and feature extraction- is on-line achieved. Classification algorithms have been implemented by Artificial Intelligence techniques, using NEXPERT OBJECT expert system.

A general architecture is shown for applying in surface inspection problems. It achieves: high performance, flexibility, possibility of multi-sensor integration, modularity. These characteristics make

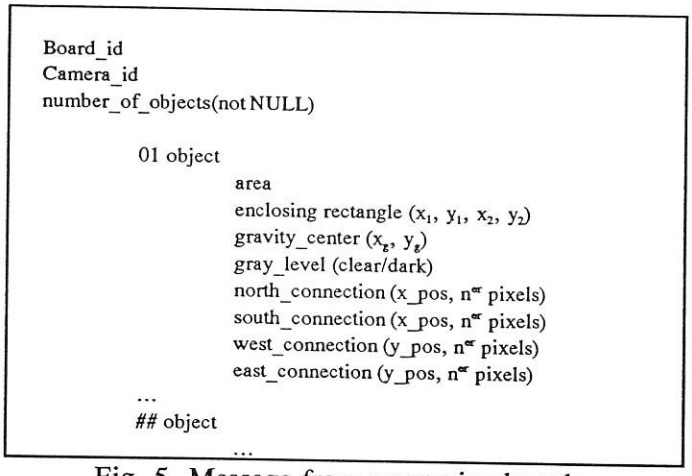

Fig. 5. Message from processing boards.

it suitable for many surface inspection tasks, not only aluminum strip. It can apply to wood surfaces, metal surfaces, plastic surfaces,... with little effort on both equipment changes and software development.

The exposed system constitutes a substantial improvement of a very cost-effective industrial process that is aluminum strip obtention by means of continuous casting.

6 References

[1] Freeman, H. Machine vision for inspection and measurement. Academic Press, 1989.

[2] Roland T. Chin. "Automated visual inspection: 1981 to 1987". CVGIP 41, pp 346-381, 1988.

[3] Jain, A.K. Fundamentals of digital image processing. Prentice Hall, 1989.4. Gonzalez, R.C. and Safabakhsh, R. "Computer vision techniques for industrial inspection and robot control: A tutorial overview". IEEE EH0241-0/86/0000/0400$01.00. 1986.

[4] Hall, R. Illumination and color in computer generated imagery. Springer-Verlag, 1989.

[5] IEEE Proceedings 22nd. International Symposium on Industrial Robots. October 21-29 1991. Detroit, Michigan.

[6] Jain, A.K. Real-time object measurement and classification. Springer-Verlag, 1987.

[7] Bechmann, P., Spizzichino. The Scattering of Electromagnetic Waves from Rough Surfaces, New York, Pergamon, 1963.

[8] Torrance, K., Sparrow, E. "Off-specular peaks in the directional distribution of thermal radiation". J. Heat Transfer, pp. 223-230, May 1966.

[9] Torrance, K., Sparrow, E. "Theory off-specular reflection from roughness surfaces". J. Opt. Soc. Amer. nº 57, pp. 1105-1114, 1967.

[10] Haralick, H. "Statistical and structural approaches to texture". Proceedings of the IEEE, vol 67 nº5 1979, pp 786-804.

[11] Tamura, H. and Mori, S. "Textural features and visual perception". IEEE Trans. on Systems, Man and Cybernetics vol SMC-8 nº 6 June 1978.

[12] Lee, C. and Chao, Y.J. "Surface texture dependence on surface roughness by computer vision". IEEE CH2413-3/87/0000/5220$01.00, 1987.

[13] Gonzalez, R.C., Wintz, P. Digital Image Processing. Addison-Wesley 1987.

[14] Patrick, E.A. Fundamentals of pattern recognition. Prentice Hall, 1972.

[15] Fu, K. Robotics: Control, Sensing, Vision and Intelligence. McGraw Hill, 1988.

[16] Banks, S. Signal Processing Image Processing and Pattern Recognition, Prentice Hall, 1990.

[17] Feldman, J.A. "Some decidability results on grammatical inference and complexity". Inf. Control, 20, 244-46, 1972.

[18] Platero, C., Fernandez, C. Deteccción y Clasificación de Defectos en Planchas de Aluminio, mediante Visión Artificial. Servicio de Publicaciones de la E.T.S.I.I., Madrid, 1992.